RESEARCH ARTICLE

Enhancement of Solubility of Anti-Inflammatory Drug By Using Different Solubility Enhancement Techniques

Naresh Kumar Dhinwa, Yuvraj Singh Sarangdevot, Chetan Singh Chauhan, Bhupendra Vyas*
Faculty of Pharmacy, Bhupal Nobles' University, Udaipur (Rajasthan), india-313001

Received: 21st Sep, 2024; Revised: 22nd Oct, 2024; Accepted: 15th Nov, 2024; Available Online: 25th Dec, 2024

Abstract
Celecoxib (CXB) is classified as a Class II molecule in the Biopharmaceutical Classification System (BCS), characterized by high permeability but low solubility in water. This limited solubility results in variable absorption and reduced bioavailability when taken orally. To address these challenges, dry co-milling technology, which is suitable for industrial applications, can be employed. This study aimed to develop and optimize nanoformulations of CXB using dry co-milling technology, applying a quality by design approach to enhance solubility, dissolution rate, and oral bioavailability.
Keywords: Celecoxib, Antiinflammtory, solubility technique
How to cite this article: Naresh Kumar Dhinwa, Yuvraj Singh Sarangdevot, Chetan Singh Chauhan, Bhupendra Vyas Enhancement of Solubility of Anti-Inflammatory Drug By Using Different Solubility Enhancement Techniques. International Journal of Pharmaceutical Quality Assurance. 2024;15(4): 2543-57. doi: 10.25258/ijpqa.15.4.55
Source of support: Nil
Conflict of interest: None

INTRODUCTION

As a highly debated yet not fully settled topic, techniques for enhancing solubility or dissolution continue to be a dynamic area of research within formulation science. Solubility and dissolution are fundamental principles in both physical and chemical sciences, encompassing biopharmaceutical and pharmacokinetic factors relevant to the treatment of various medications. However, as synthetic methods advance and yield numerous promising lead compounds across various pharmacological categories, there is a trend towards developing larger molecular structures.

Consequently, over 40% of new candidates that enter the drug development pipeline do not succeed due to suboptimal biopharmaceutical characteristics. These characteristics, such as the rate and extent of absorption, distribution rate, and the dosage required to reach the minimum effective concentration while minimizing side effects, can greatly impact the drug's absorption, distribution, metabolism, excretion, and toxicity. Throughout the years, advancements in drug discovery tools have led to a noticeable change in biopharmaceutical properties [1, 2].

Pharmaceutical companies have mainly utilized two approaches for drug discovery: rational drug design (RDD) and high throughput screening (HTS). In both methods, lead compounds are identified through screening processes that consider their interaction with biological systems. RDD typically produces compounds with greater molecular weight, which can lead to reduced permeability [3].

Numerous strategies are employed to enhance dissolution, absorption, and consequently, in vivo effectiveness by addressing the solubility challenges associated with drugs that exhibit low bioavailability. To improve the solubility and dissolution rate of these drugs, it is essential to increase the surface area of the active ingredient that interacts with the surrounding liquid. Various techniques are utilized for this purpose, including the formation of cyclodextrin complexes, the preparation of solid dispersions, microemulsion techniques, and methods for reducing particle size. Particle size reduction techniques can be categorized into two main groups: mechanical methods and engineering-based size control methods. Mechanical particle size reduction, also known as micronization or nanonization, involves the use of jet mills, high-energy ball mills, and planetary ball mills, along with high-pressure homogenization techniques. Engineering-controlled methods include cryogenic spraying, which produces nano-structured amorphous particles with high porosity at extremely low temperatures, and crystal engineering, which focuses on obtaining metastable polymorphs, high-energy amorphous forms, and very fine particles through a controlled crystallization process [4].

Among the techniques discussed, mechanical particle size reduction stands out as the most applicable in industrial settings. Numerous medications benefit from this method, as it enhances their bioavailability through particle size reduction [1,13,16–18]. Conversely, the wet milling technique is employed to achieve more effective and favorable outcomes in particle size reduction. However, this method entails a complex and time-consuming process in the production of solid dosage forms, as the particles generated must be transformed into a solid state using techniques like spray drying or lyophilization [5].

This research aims to enhance the properties of submicron and nano-sized celecoxib particles through the application of dry co-milling technology, guided by a quality by design framework. A key aspect of this study is the

**Corresponding author: nareshkumardhinwa@gmail.com*

identification of optimal parameters that improve the solubility and dissolution rates of celecoxib nano formulations, which are subsequently assessed through both in vitro and in vivo studies. Additionally, this research offers a methodological advancement by showcasing the effectiveness of a cutting-edge data-driven optimization method known as Bayesian Optimization (BO), which streamlines the experimental process in comparison to traditional experimental design approaches [6].

The Central Composite Design (CCD) model plays a crucial role in Response Surface Methodology (RSM). This approach combines statistical and mathematical techniques to minimize the number of experiments by selecting optimal experimental conditions to achieve the desired product profile. The CCD model is also known as the Box-Wilson Central Composite Design. In this framework, the central points are enhanced with a set of "star points," which facilitate the assessment of curvature. Unlike factorial design, this methodology enables the identification of quadratic effects of the factors, allowing for a more comprehensive analysis of response curvature [7].

Table 1: Development of Celecoxib loaded SD

S. No.	Design of Batches in (1:1/1:1/1:1) (Drug: Polymer ratio)	Development	Solvent System	Comments
1.	Celecoxib: PVP K-30	Modified Co-evaporation method	Ethanol: water (Glacial Acetic Acid)	Successfully Develop Solid Dispersion
2.	Celecoxib: Mannitol	Solvent evaporation Method	Ethanol	
3.	Celecoxib: PEG-6000	Modified Solvent evaporation method	Ethanol: Dichloromethane	

Table 2: Percentage Yield of Physical Mixture and Solid Dispersion of Celecoxib

Sample	Weight of Solid Dispersion (mg)	Weight of Celecoxib (mg)
PMPV 1	49.1	25
PMPV 2	74.2	25
PMPV 3	124.8	25
PMMT 1	49.7	25
PMMT 2	74.5	25
PMMT 3	124.3	25
PMPG 1	27.5	25
PMPG 2	44.7	25
PMPG 3	82.4	25

Table 3: Drug Content of Physical Mixture and Solid Dispersion of Celecoxib

Sample	Celecoxib	
	Drug Content (mg)	% Drug Entrapment
PMPV 1	24.84	99.36
PMPV 2	25.12	100.48
PMPV 3	24.77	99.08
PMMT 1	25.08	100.32
PMMT 2	24.81	99.24
PMMT 3	24.68	98.72
PMPG 1	24.72	98.88
PMPG 2	24.58	98.32
PMPG 3	24.81	99.24

Table 4: Phase Solubility Study of Celecoxib in Physical Mixtures and Solid Dispersions

Preparation	Solubility of Celecoxib (mg/ml)	Gibbs Free Energy ($\Delta G_{tr}°$)
Celecoxib Pure Drug	0.246 ± 0.024	0
Physical Mixture with PVP K-30 (PMPV)	1.457 ± 0.164	-45.2443
Physical Mixture with Mannitol (PMMT)	1.915 ± 0.125	-52.1967
Physical Mixture with PEG-600 (PMPG)	1.162 ± 0.11	-114.279
Solid Dispersion with PVP K-30 (SDPV)	4.468 ± 0.23	-85.6872
Solid Dispersion with Mannitol (SDMT)	9.256 ± 0.315	-92.2713
Solid Dispersion with PEG-600 (SDPG)	7.145 ± 0.278	-148.535

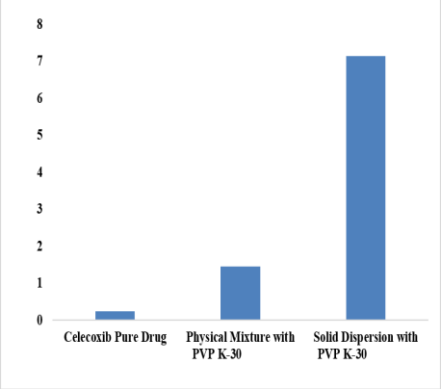

Phase Solubility Study of Celecoxib in Physical Mixtures and Solid Dispersions with PVP K-30

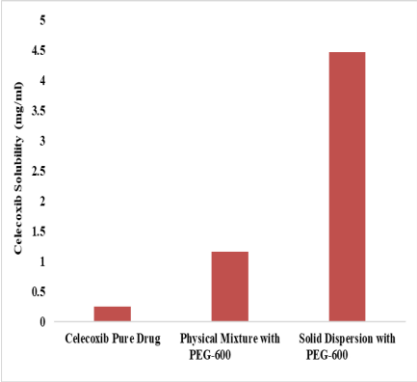

Phase Solubility Study of Celecoxib in Physical Mixtures and Solid Dispersions with PEG-600

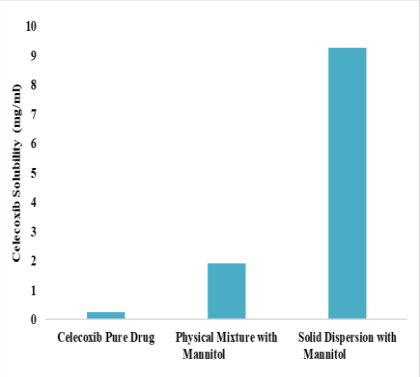

Phase Solubility Study of Celecoxib in Physical Mixtures and Solid Dispersions with Mannitol

Table5: Invitro Drug Dissolution Data for Celecoxib Pure Drug and Physical Mixtures and solid dispersion of celecoxib with PVP K-30, mannitol and PEG-6000

Time (Mins)	Celecoxib		PMPV 1		PMPV 2		PMPV 3		PMMT 1		PMMT 2		PMMT 3		PMPG 1		PMPG 2		PMPG 3	
	%CDR	± SD	% CDR	± SD	% CDR	± SD	% CDR	± SD	% CDR	± SD	% CDR	± SD	% CDR	± SD	% CDR	± SD	% CDR	± SD	% CDR	± SD
0	0	0	0	0	0	0	0	0	0	0	0	0	0	0	0	0	0	0	0	0
10	11.58	1.59	8.01	1.06	10.99	1.58	7.87	1.31	17.94	2.33	20.32	3.72	20.7	3.20	14.54	3.98	17.07	3.62	15.04	2.82
20	20.78	2.28	14.24	1.14	20.38	4.58	20.05	2.75	31.83	3.14	41.13	5.64	41.13	2.14	26.35	4.45	29.94	3.13	36.32	3.66
30	29.57	1.03	22.69	3.20	33.46	6.90	29.67	4.26	45.11	4.74	56.89	2.48	64.73	4.94	36.81	5.01	44.08	3.59	57.74	3.89
40	39.93	2.3	37.84	5.66	45.14	5.83	47.89	7.53	59.87	5.66	72.54	2.71	89.99	4.69	47.93	4.71	60.58	2.69	71.66	5.57
50	48.41	0.56	52.15	5.58	55.41	3.70	64.25	5.27	70.17	3.60	86.45	4.16	100.06	4.69	60.81	5.66	74.22	3.54	88.08	2.69
60	56.41	1.7	66.06	5.38	66.85	5.35	73.1	3.40	79.61	5.07	100.19	1.45	--	--	71.83	3.01	88.9	3.08	100.21	1.07
70	63.61	3.3	73.17	5.27	76.14	4.42	82.7	2.15	88.35	3.05	--	--	--	--	83.02	4.22	100.27	0.39	--	--
80	75.16	2.71	80.59	5.52	85.31	6.30	92.32	2.75	100.59	2.16	--	--	--	--	92.93	2.37	--	--	--	--
90	84.91	1.21	89.62	2.46	93.92	5.96	97.89	1.45	--	--	--	--	--	--	100.68	0.52	--	--	--	--
100	91.86	1.77	95.05	1.88	100.37	1.10	100.85	0.95	--	--	--	--	--	--	--	--	--	--	--	--
110	97.79	1.33	100.61	0.64	--	--	--	--	--	--	--	--	--	--	--	--	--	--	--	--
120	101.23	1.03	--	--	--	--	--	--	--	--	--	--	--	--	--	--	--	--	--	--
t 90 %	**100.22**		**92.09**		**85.41**		**80.79**		**98.31**		**93.85**		**90.42**		**77.76**		**69.39**		**52.2**	
P Value	**--**		**0.16**		**0.008**		**0.004**		**0.03**		**0.023**		**0.004**		**0.0003**		**0.002**		**0.003**	

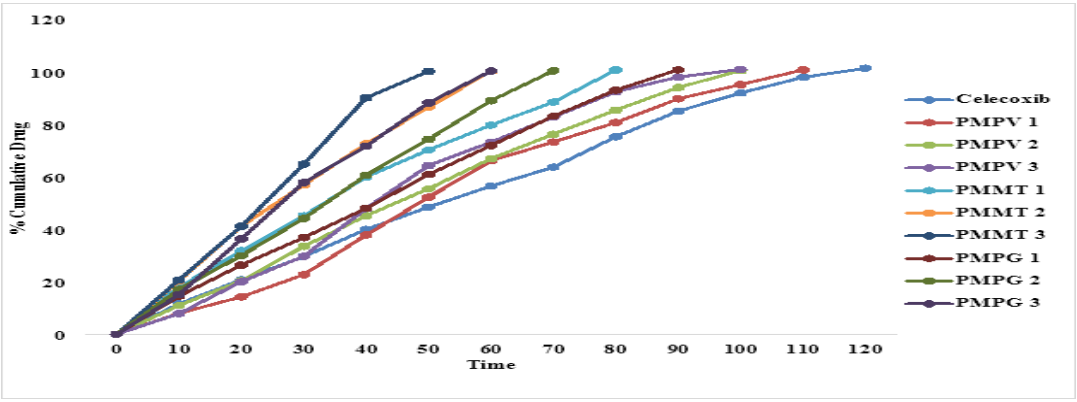

Figure 1: Comparative In-Vitro Drug Release Profile of Celecoxib Pure Drug andPhysical Mixture (Celecoxib)

Table 6: DSC Peaks of Celecoxib & PEG-6000, SDPMPG2 and SDPMPG3

Sample	Peak (ºC)	Inference
Celecoxib	266	Melting Endotherm
PEG-6000	168	Melting Endotherm
SDPMPG2	120	Endothermic peak corresponding to melting of Celecoxib absent in prepared solid dispersion
SDPMPG3	160	Endothermic peak corresponding to melting of Celecoxib absent in prepared solid

dispersion

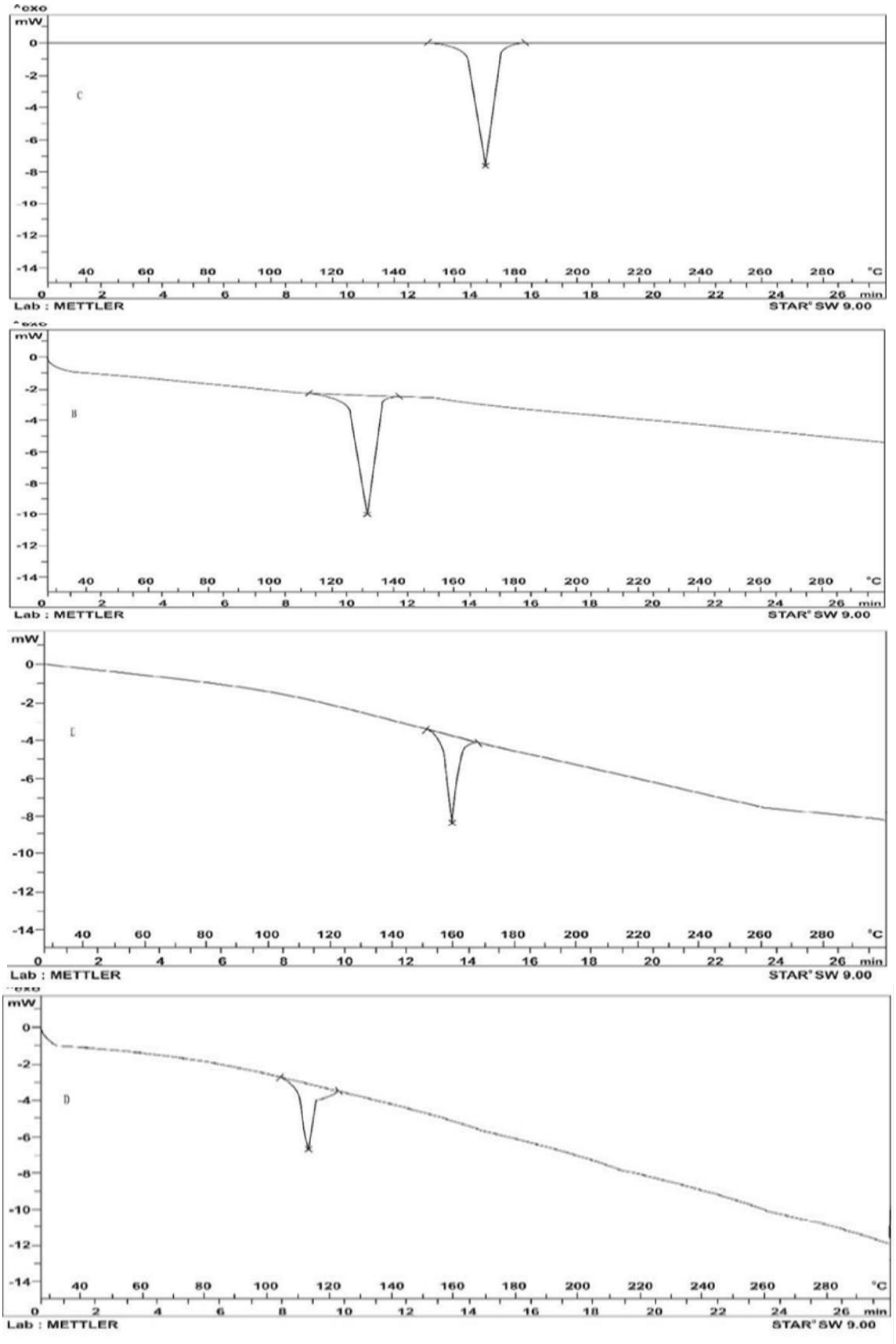

Figure 2: Overlay DSC Thermograms of (A) Celecoxib, (B) PEG-6000, (C) SDPMPG2, and (D) SDPMPG3

Table 7: XRD Data for Celecoxib Pure Drug

Angle, 2 - Theta°	d – value, Angstroms	Intensity %	Angle, 2 - Theta°	d – value, Angstroms	Intensity %
10.749	8.22367	56.1	21.666	4.09849	42.1
12.097	7.3106	39.4	22.524	3.9442	25.6
14.42	6.13767	35.3	23.303	3.81412	64.6
15.138	5.84798	26.3	23.803	3.73521	39.9
16.004	5.53355	50.9	24.139	3.68389	59.1
16.714	5.30006	74.8	24.771	3.59128	48
17.057	5.19409	25.8	25.434	3.49926	24.1
18.279	4.84968	53.3	25.964	3.42893	21.4
18.786	4.71985	35.8	26.364	3.3778	20.9
19.246	4.60809	52.2	28.052	3.17835	24.4
19.61	4.52328	100	28.936	3.08314	21.8
20.61	4.30609	76	29.493	3.02618	19.8
20.971	4.23268	52.9	34.364	2.60756	21.2

Table 8: XRD Data for Solid Dispersions SDPMPG2 and SDPMPG3

SDPMPG2			SDPMPG3		
Angle, 2 - Theta°	d – value, Angstroms	Intensity %	Angle, 2 - Theta°	d – value, Angstroms	Intensity %
10.79	8.12514	36.90346	10.816	8.2398	22.33151
12.091	7.2943	29.18033	11.219	7.6745	34.42623
12.297	7.1362	30.96539	11.394	7.4621	22.36794
14.432	6.0746	26.99454	12.406	7.2546	20.07286
16.014	5.416	27.35883	12.586	7.1843	28.56102
16.718	5.2746	31.76685	13.794	6.487	31.11111
16.798	5.1894	27.79599	14.424	5.926	19.89071
18.815	4.2451	22.55009	18.768	5.1035	21.45719
19.198	4.6016	23.49727	19.213	4.602	21.63934
19.246	4.5487	23.02368	19.748	4.2164	28.74317
19.44	4.5418	21.38434	20.116	4.117	37.12204
19.63	4.5119	30.01821	20.192	4.0862	23.82514
19.642	4.3476	40.07286	23.303	3.826	21.38434
23.303	3.7541	25.93807	23.384	3.719	23.13297
24.144	3.5638	22.36794	24.546	3.3216	20.47359

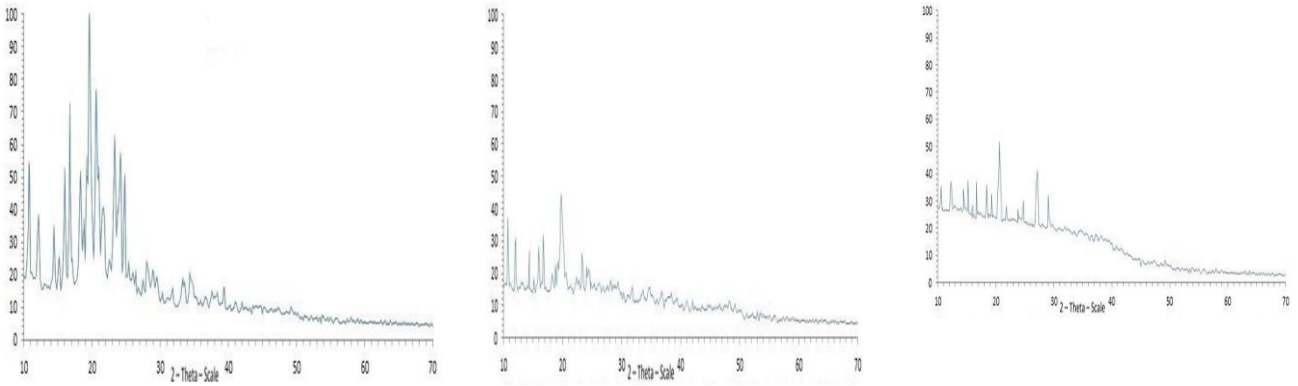

Figure 3: Overlay XRD Spectra of Celecoxib Pure Drug, SDPMPG2 & SDPMPG3

Table 9: No. of Peaks and % Crystallinity Details of XRD Study of Celecoxib Pure Drug, SDPMPG2 & SDPMPG3

Sample	No. of Peaks	% Crystallinity
Celecoxib	32	100
SDPMPG2	18	50.82
SDPMPG3	15	42.86

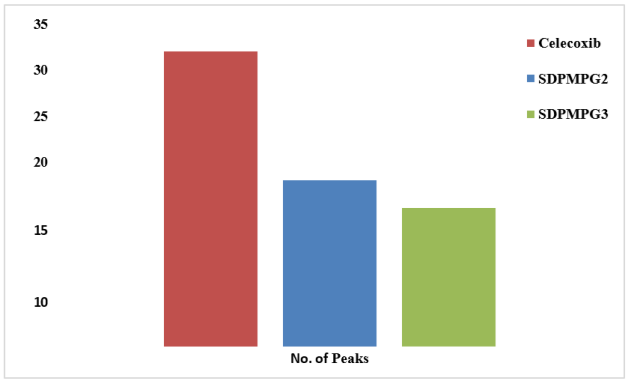

No. of Peaks Comparative Bar Graph of Celecoxib Pure Drug, SDPMPG2 & SDPMPG3

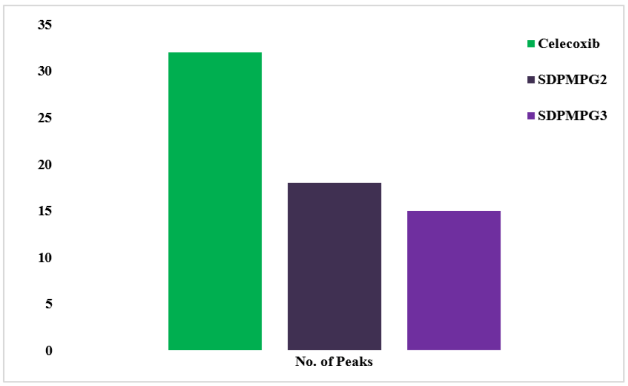

% Crystallinity Comparative Bar Graph of Celecoxib Pure Drug, SDPMPG2 & SDPMPG3

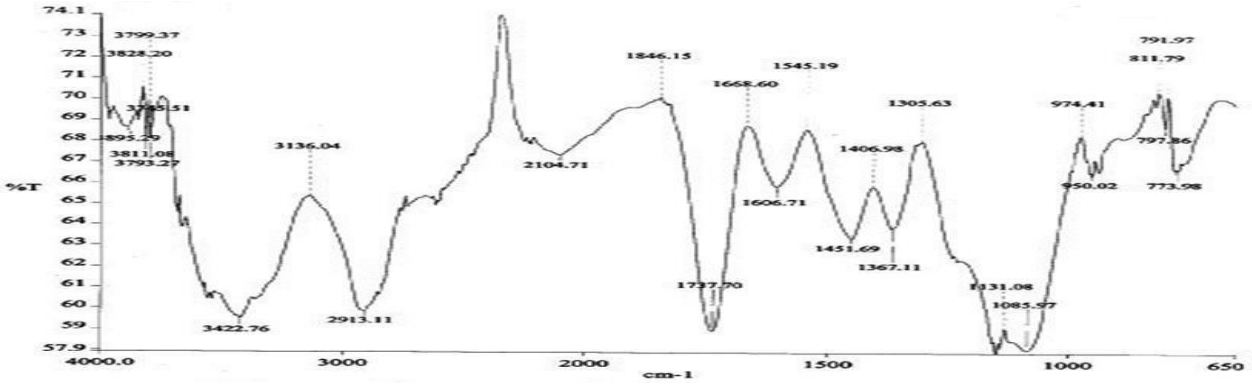

Figure 4: FTIR Spectra of Celecoxib SD

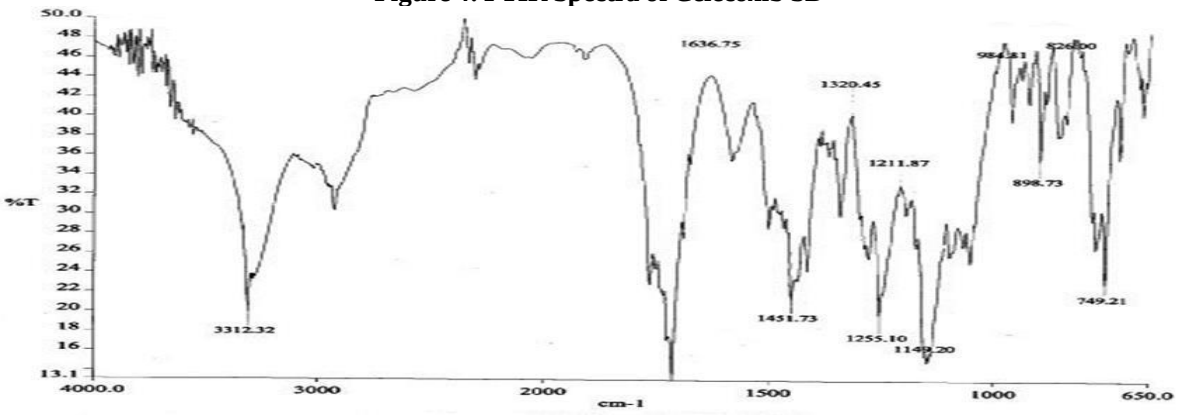

Figure 5: FTIR Spectra of Celecoxib PM

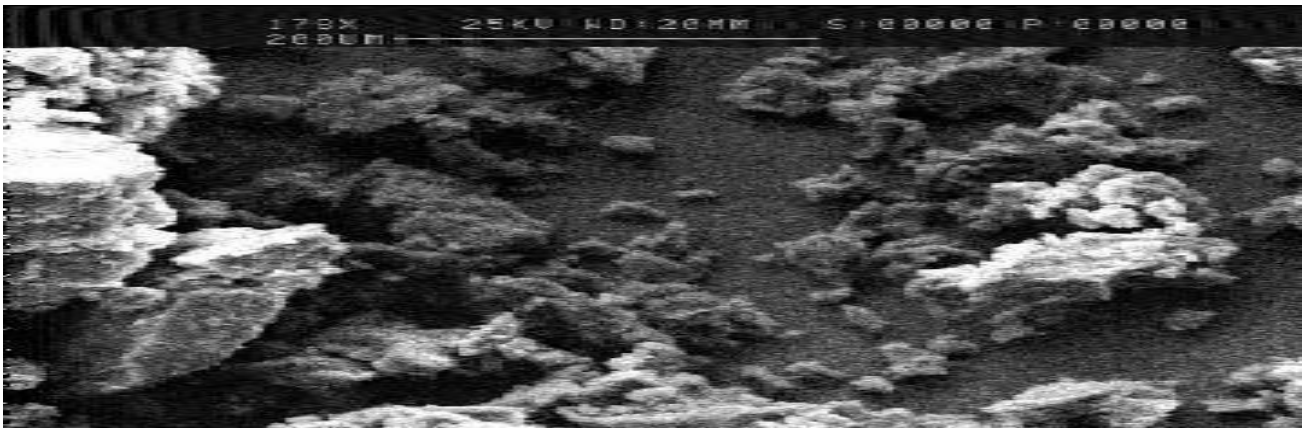

Figure 6: SEM of PEG-6000

A **B** **C**

Figure 7: Scanning electron microphotographs of (a) Celecoxib alone, (b) Physical mixture of Celecoxib-PEG-6000 binary systems, (c) Solid dispersion of Celecoxib.

Table 10: Flow Properties of Solid Dispersion of Celecoxib

Property	SDPMPG2	SDPMPG3
Angle of Repose	37.56	39.05
Bulk Density	0.4149	0.4037
Tapped Density	0.5364	0.5387
Carr's Index	22.65	25.06
Hausner's Ratio	1.29	1.3344

Table 11: Flow Properties of Granules of Solid Dispersions of Celecoxib

Property	SDPMPG2	SDPMPG3
Angle of Repose	25.3	26.12
Bulk Density	0.4762	0.4648
Tapped Density	0.5474	0.5341
Carr's Index	13	12.98
Hausner's Ratio	1.1495	1.1491

Table 12: Physical Parameters of Tablets of Solid Dispersions of Celecoxib

Property	TSDPMPG2	TSDPMPG3
Hardness (Kg/cm^2)	4.89 ± 0.26	4.56 ± 0.12
Friability in %	0.89	0.66
Disintegration Time (Mins)	5.15	4.58
Weight variation (mg)	152.701 mg ± 3.38	151.85 mg ± 5.54
Average Drug Content (mg)	25.13 mg ± 0.79	25.49 mg ± 0.95
Average table weight (mg)	77.12 ± 5.54	131.47 ± 3.38

Time (Mins)	Celecoxib					
	Marketed Celecoxib		TSDPMPG2		TSDPMPG3	
	% CDR	± SD	% CDR	± SD	% CDR	± SD
0	0	0	0	0	0	0
10	9.47	3.21	20.82	3.85	18.09	4.50
20	19.91	3.78	41.42	4.56	35.60	2.84
30	28.31	4.25	65.17	3.89	55.86	5.95
40	41.64	4.67	90.28	5.84	71.66	4.69
50	51.63	4.85	101.22	2.01	88.22	4.51
60	61.06	5.45	--	--	100.61	2.12
70	69.50	3.64	--	--	--	--
80	78.58	4.15	--	--	--	--
90	87.59	3.69	--	--	--	--
100	94.73	2.89	--	--	--	--
110	100.67	3.14	--	--	--	--

120	--	--	--	--	--	--
t 90 %	**96.46**		**42.48**		**51.75**	
P Value	**--**		**0.009**		**0.003**	

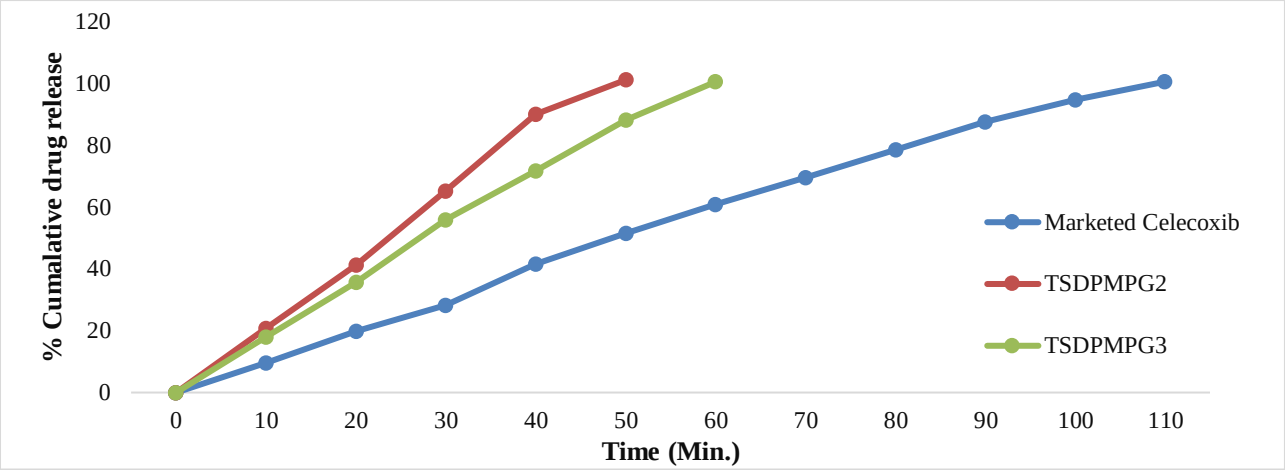

Figure 8: Comparative *in-vitro* Drug Dissolution Profile of Solid Dispersion Tablets of Celecoxib & Celecoxib Marketed Tablet (Celecoxib)

Table 13: Comparison of drug release after 6 months

Temp (ºC)/ RH (%)	Time (months)	Appearance	Particle size* (nm)	PDI*	Zeta Potential* (mV)	Drug content (mg/ml)
$40^0C \pm 2^0C$/ 75% Rh±5%Rh	0	White	108.5 ± 2.1	0.172±0.003	-21.2±1.9	25
	1	White	109.2 ± 1.9	0.175±0.007	-21.1±2.0	25
	2	White	109.9 ± 2.0	0.181±0.009	-20.9±1.5	25
	3	White	110.5 ± 1.5	0.182±0.005	-21.4±1.4	25
	4	White	111.7±1.9	0.183±0.008	-21.2±1.6	25
	5	White	111.9±1.6	0.184±0.006	-21.1±1.7	25
	6	White	112.4±1.6	0.185±0.002	-21.2±1.5	25

The CCD models, along with traditional experimental design frameworks, outline the specific experiments to be conducted, their order, and the number of repetitions prior to initiating the experiments. In contrast, Bayesian Optimization (BO) employs an iterative, data-driven methodology for selecting experiments and enhancing the response variable. BO systematically identifies which new experiments will yield the most valuable insights based on the outcomes of prior experiments. Unlike CCD, the number of experiments in BO is not predetermined; the iterative optimization continues until the optimal solution is achieved. BO is particularly effective for optimizing black-box functions that are costly to evaluate. It has demonstrated the ability to efficiently identify optimal solutions with a limited number of experiments across various fields, including material science and machine learning.

In this study, CXB was utilized as the active pharmaceutical ingredient. CXB is a selective inhibitor of cyclooxygenase-2 and is among the frequently prescribed nonsteroidal anti-inflammatory drugs (NSAIDs) for both acute and chronic management of symptoms associated with rheumatoid arthritis, osteoarthritis, ankylosing spondylitis, and pain relief. Classified as BSC Class II, CXB exhibits low aqueous solubility (5 µg/mL at temperatures between 5–40 °C) alongside high permeability. Its solubility remains consistent below pH 9.0 and increases at pH 12 [8].

Materials and Methods

Solubility Enhancement and Formulation Development of Celecoxib by Solid Dispersion Approach

The goal of the current study is to create solid mixtures of celecoxib (CXB) using PVP-K30, PEG-6000, and mannitol as carriers by a variety of techniques, including solvent evaporation (SE), kneading (KT), and physical mixing (PM). This chapter examined and reported on the many parameters used in the preparation and assessment [9].

Preparation of solid mixtures

Using three distinct methods physical mixing, kneading, and solvent evaporation solid mixes of the chosen medications, celecoxib with polyvinyl pyrrolidone (PVP K-30), PEG-6000, and mannitol as carriers, were made for the current study. For celecoxib, solid mixes were made with PVP-K 30, PEG-6000, and mannitol in drug to carrier weight ratios of 1:1, 1:1, and 1:1, respectively. All three of the approaches employed in this inquiry used the same ratios [10].

Physical mixture preparation

Simple mixing of precisely weighed amounts of medication and the carriers sorted through sieve #100 in a closed glass bottle produced physical combinations. After

that, the powders were kept in a desiccator. Five grammes of the physical combination were made in each instance.

Preparation of kneading mixtures

In a mortar, weighed amounts of the medication and carrier were triturated with a tiny amount of methanol. After 45 minutes of kneading, the thick slurry was dried to constant weight at 50°C. The desiccator was used to hold the dry mass after it had been ground up and sieved via sieve #100. Five grammes of the kneading mixture were made for each case [11].

Preparation of solid dispersions using solvent evaporation technique

Solvent evaporation was used to create solid dispersions of the chosen medication, celecoxib. To get a transparent solution, the right amounts of medication and polymer were dissolved in about 60 ml of solvent blend. The solvent blend for PVP-K-30, PEG-6000, and mannitol was a 2:1 mixture of dichloromethane and methanol. Next, the solvent mixture was eliminated by evaporation in a water bath at 45° C with lowered pressure. After that, the residue was moved to a glass desiccator and vacuum-dried to a consistent weight. Before being used, the dry product was ground into a powder, sieved through sieve #100, and kept in a desiccator. Five grammes of dispersion were made for each instance [12].

Evaluation of Solid dispersions

The solid dispersions prepared were evaluated for drug content uniformity, in vitro drug release studies.

Drug content uniformity

Four 100 mg samples were obtained from each batch of the solid combinations that were made, and their drug concentration was examined. To make it easier to extract the medication from the solid combination into solvent, 100 mg of the mixture was weighed into a 50 ml volumetric flask, diluted with methanol, and thoroughly mixed before being set aside for four hours with periodic shaking. After being brought to volume, the solution was passed through a 0.45µm membrane filter (Millipore nylon discs). Celecoxib's drug concentration was determined by spectrophotometrically evaluating the absorbencies of the solutions after they had been appropriately diluted further. Celecoxib's mean drug content and coefficient of variation [13].

Interference Study

By evaluating each polymer's effects separately for Celecoxib, the interference caused by the polymers employed in this experiment was examined. Celecoxib, PVP-K30, PEG-6000, and mannitol in a 1:1 ratio were all carefully combined in precisely weighed proportions. Using the previously mentioned procedure, a precisely weighed powder containing 50 mg of Celecoxib was extracted from each mixture. The calibration curve was used to determine the celecoxib contents [14].

Drug release studies

Dissolution tests were conducted using the paddle method at a rotation speed of 50 rpm, with three separate tests performed for both pure drugs and solid mixtures using the USP XXIV Dissolution Rate Test Apparatus (Lab India Disso 2000). For celecoxib, preparation samples equivalent to 60 mg of the drug were placed into hard gelatin capsules and added to the dissolution medium. For another preparation of celecoxib, a 100 mg drug equivalent was spread directly on the dissolution medium. At regular intervals, 5 ml samples were withdrawn, and the samples were filtered using a 0.45 µm membrane filter (Millipore nylon discs). Five milliliters of the dissolving media were added to maintain the starting volume. After being appropriately diluted, the filtered solutions were spectrophotometrically tested for drug concentration by comparing their absorbencies to a blank. The standard deviation and mean percentage of medication dissolved were computed [15].

Comparison of dissolution profiles and drug release mechanisms and kinetics of dissolution rate

Several methods, including analysis of variance based, model-independent, and model-dependent approaches, can be used to mathematically compare dissolution data in order to quantify observed changes in the rate and extent of drug release as impacted by formulation and process variables. Statistically significant variations in dissolution profiles can be found using ANOVA procedures, which are frequently employed to identify significant changes between groups. The mean dissolution time or the ratio of the area under the dissolution curve (dissolution efficiency) are the foundations of model-independent methods. In the model-dependent approaches, the release kinetics and release mechanism are evaluated by fitting the individual dissolution data with mathematical models. Despite the difficulties and restrictions associated with each of these approaches, the numerical figures they produce can be used as quantitative measurements to compare the complete dissolution profiles and to describe the kinetics and mechanisms of drug release [16].

Model-independent approaches

Comparing the time required for a specified percentage of the active drug to dissolve in the dissolution medium can be done using parameters such as T50 and T90. These values represent the time at which 50% and 90% of the drug, respectively, has dissolved. Another key parameter is Dissolution Efficiency (DE), which is determined as a model-independent method. DE is calculated as the area under the dissolution curve up to a given time (t), expressed as a percentage of the area of a rectangle that represents 100% dissolution at the same time. This provides an overall measure of the efficiency of the dissolution process.

$$DE_8\% = \frac{\int_0^t y\,dt}{y_{100}\,t} \times 100$$

The dissolution efficiency (DE) can vary depending on the selected time period. However, it is important to use consistent time intervals for comparison. For example, the dissolution efficiency of a drug from a specific formulation after 30 minutes is represented by the index DE30, which can only be compared to DE30 of other formulations. To simplify the comparison across multiple formulations, a single DE value summarizing the drug dissolution data is helpful. From the dissolution data of each formulation, values such as DE10 and DE20 can be calculated and used for comparison. The dissolution parameters for all solid

celecoxib formulations include T50, T90, DE10, and DE20 [17].

Zero order release kinetics

$$Qt = Q_0 + K_0t$$

Here, Ko represents the dissolution rate constant for zero-order release, and Q(t) signifies the percentage of the drug dissolved as a function of time (t) in minutes. If the drug follows zero-order release kinetics, the plot of drug release versus time will yield a straight line. The slope of the graph, which plots the percentage of drug released against time, is used to determine the dissolution rate constant (Ko) for each formulation.

First order release kinetics

$$\ln (100-Q) = \ln Q_0 - K_1t$$

A regression coefficient (R^2) closer to 1 indicates that the drug release follows first-order kinetics, meaning the release is concentration-dependent. This value is obtained by plotting the logarithm of the percentage of the remaining drug to be released (log% ARR) against time. If the plot is linear and the R^2 value is high, it suggests that the release follows first-order kinetics [18].

Higuchi Square Root of Time Model

$$Q = Kht^{1/2}$$

Higuchi's drug release model suggests Fickian diffusional release, as indicated by the regression coefficient of percentage drug release vs square root of time that is closer to 1 [19].

Hixon-Crowell Cube Root Model

$$\sqrt[3]{Q_0} - \sqrt[3]{Q_t} = KHC.t$$

R^2 values nearer to 1 for the plot of amount of drug released versus cube root time indicate Hixon – Crowell model [20].

Korsmeyer And Peppas Model

$$Q_t / Q_\infty = K \times t^{\lambda}$$

$$\text{Log}\,(Q_t/Q_\infty) = \text{Log}\,K + \Lambda\,\text{Log}\,t$$

A plot of log (Q_t/ Q_∞) versus log t gives straight line of gradient λ and an intercept of log K. Values of exponent Λ and the corresponding release mechanism [21].

Solid state studies

Fourier transform infra-red (FT-IR) analysis

A FT-IR spectrophotometer (JASCO FT/IR-4200 Spectrophotometer) in Tokyo, Japan was used to measure the FT-IR spectra of pure drugs, physical mixtures, and solid dispersions in the wave number range of 4000-400 cm-1 [22].

Differential scanning Calorimetry study

A Shimadzu DSC-60 differential scanning calorimeter with a thermal analyser, located in Tokyo, Japan, was used to conduct the DSC measurements. In hermetically sealed aluminium pans, precisely weighed samples (about 5–10 mg) were heated in a nitrogen environment at a flow rate of 20 ml min–1 and a scanning rate of 15 °C min– 1 between 60 and 250 °C. The reference was an empty aluminium pan [23].

X-ray diffraction study

The X-ray powder diffraction method was used to assess the crystalline condition of several samples. With minor adjustments, the X-RD analysis of the pure drug, best formulations S2, S22, and physical mixture W2 and W22 was carried out at the Centre for Earth Studies, Thiruvanthpuram, using the procedure described by Li et al., [108]. A Philips Analytical X-ray BV 1710 with a graphite monochromator and cobalt as the anode material was used to obtain the diffraction patterns at ambient temperature while operating at a voltage of 30 kV. The process parameters were set at a scan rate of 0.020 seconds-1, and the samples were examined within the 2θ angle range of 10 to 500 [24].

Scanning electron microscopy (SEM)

Drug-SD surface morphology was studied under scanning electron microscope (SEM) at JNU, New Delhi using polymer HPMC-AS (S2, S22) and PM (W2, W22). Prior to this, the samples were fixed on alumina stubs with double adhesive tape, sputtered with gold in a Hitachi HUS-GB vacuum coating unit and visualized in a Hitachi S- 300 N Scanning electronic microscope at 10 Kv voltage [25].

Drug Content

SDs equivalent to 50 mg of drug was accurately weighed and dissolved in 50 ml of Phosphate buffer pH 7.4. The stock solutions were filtered. (The solutions were subsequently diluted appropriately in the same solvent). The drug content was estimated at 230 and 360 nm with a UV spectrophotometer (shimadzu-1700 series) triplicates were taken for each sample [26].

Percentage yield

The amount of product actually produced by the reaction is the actual yield and will usually be less than the theoretical yield. To express the efficiency of a reaction, it is often calculating the percent yield, which is defined by:

$$\% \text{ yield} = \frac{\text{actual yield}}{\text{Theoretical yield}} \times 100$$

Determination of in vitro drug release of solid Dispersions

Procedure of Dissolution Study

The in vitro drug dissolution studies were performed for the drug, PM and SD by the USP paddle method using the dispersed powder technique. 500 ml of 6.8 phosphate buffer at 37^0C was added to 50mg drug sample and mixed for 75 rpm. At different intervals of time, the volume of dissolution medium was withdrawn and replaced with an equal volume of fresh dissolution medium (at same temperature) to maintain the volume constant. The samples were filtered through Millipore membrane of 0.45 µm pore diameter and were estimated for the drug content spectrophotometrically at 230 and 360 nm [27].

Dissolution Parameters

Medium : Phosphate buffer (pH= 7.4)
Type : USP apparatus I (paddle) type
RPM : 75
Quantity : 900ml
Temperature : 37± 0.2°C
Duration : 1 hr
Sampling time: 10 min, 20min, 30min, 40min.50min and 60 min.

STABILITY STUDY

The stability study was carried out for optimized

formulation as per ICH guidelines. The solid dispersions were placed in screw capped glass container and stored at ICH storage ($40^0C \pm 2^0C$ / 75% Rh ± 5% Rh) condition for a period of 180 days. The samples were analyzed for physical appearance and for the drug content [28].

Results and Discussion

Development of Solid Dispersion

Solid dispersion of Celecoxib was design and develop in presence of suitable hydrophilic polymer as a carrier by modification in formulation method to obtain physically and chemically stable amorphous solid dispersion by simple, quick, inexpensive and reproducible manner. These methods deal with the challenge of mixing a carrier and a drug preferably on a molecular level.

Characterization of the SD Formulations

Percentage Yield and Drug Content Analysis of Physical Mixture and Solid Dispersion of Celecoxib with PVP K-30, Mannitol, and PEG-6000

The percentage yield for both the physical mixtures and solid dispersions was determined using the appropriate formula. For the physical mixtures, the yield ranged from 96.58% to 99.84%, while for the solid dispersions, the yield ranged from 55% to 67.21%. Drug content analysis was also performed and yielded satisfactory results. The drug content in the prepared physical mixtures was found to be between 98.24% and 100.48%, while the drug content in the solid dispersions ranged within the same range. These findings regarding percentage yield and drug content are summarized in

Phase Solubility Study of Physical Mixture and Solid Dispersion of Celecoxib with PVP K-30, Mannitol and PEG-6000

Solubility Studies were carried out for Celecoxib pure drug, prepared physical mixtures and solid dispersions of Celecoxib with and Mannitol by Higuchi and Connors method as described. The equilibrium solubility of Celecoxib increased significantly in presence of Mannitol and PEG 6000".

The equilibrium solubility of pure celecoxib was found to be 0.246 ± 0.024 mg/ml. However, in the physical mixtures, the solubility significantly increased, with values of 1.457 ± 0.164 mg/ml for PVP K-30 and 1.915 ± 0.125 mg/ml for Mannitol. For solid dispersions, the increase in solubility was even more pronounced, with values of 7.145 ± 0.278 mg/ml for PEG-6000 and 9.256 ± 0.315 mg/ml for Mannitol.

To further validate these findings, Gibb's free energy (ΔGtr°) was calculated. All ΔGtr° values were negative, indicating the spontaneous nature of drug solubilization. The values also decreased with an increase in the concentration of the carriers, demonstrating that the solubilization process became more favorable as the concentration of the carriers increased.

These results suggest that the primary mechanisms responsible for increasing the solubility of celecoxib in solid dispersions, compared to the pure drug, are enhanced wettability, a change in crystallinity, and the solvent effects of PEG-6000 and Mannitol on celecoxib. The detailed results are summarized in Table 4, with graphical representations.

In-Vitro Drug Dissolution Study of Physical Mixtures and Solid Dispersions of Celecoxib with PVP K-30, Mannitol, and PEG-6000

An in-vitro drug dissolution study was performed with pure celecoxib and its physical mixtures and solid dispersions with PVP K-30, mannitol, and PEG-6000 in three different ratios: 25 mg:25 mg, 25 mg:50 mg, and 25 mg:100 mg, as described in the method earlier. The dissolution profiles obtained were used to develop appropriate equations, and the time required to release 90% of celecoxib (t90%) was calculated.

The results indicated a significant increase in the in-vitro dissolution rate for the solid dispersions. The dissolution data are summarized in Table 5, while the in-vitro release profile is presented in Figure 1 also illustrates the effect of carrier concentration on drug release and t90%. It was observed that with increasing carrier concentration, the t90% decreased.

For the pure drug, the in-vitro dissolution was very low due to its limited solubility. The t90% for the pure celecoxib drug was found to be 100.22 minutes. In contrast, for the physical mixtures prepared with mannitol, t90% ranged from 92.09 minutes for PMMT1 to 98.31 minutes for PMMT2, and 90.42 minutes for PMMA3. The t90% for physical mixtures with PEG-6000 (PMPG) showed more significant improvements: 90.42 minutes for PMPG1, 69.39 minutes for PMPG2, and 52.2 minutes for PMPG3. The slight increase in dissolution observed in the physical mixtures might be due to the solvent effect of both PEG-6000 and mannitol.

The dissolution profile for the solid dispersions showed a much more pronounced increase ($p < 0.0125$) in the dissolution rate, primarily due to the amorphization of celecoxib in the presence of PVP K-30, mannitol, and PEG-6000. The t90% for solid dispersions with PEG-6000 decreased significantly: 77.76 minutes for PMPG1, 69.39 minutes for PMPG2, and 52.2 minutes for PMPG3.

These results suggest that PEG-6000 was effective in enhancing the solubility and dissolution of celecoxib, similar to hydrophilic carriers. However, the difference in t90% between formulations prepared with PEG-6000 was not significant. This non-significant difference justifies the use of a hydrophilic drug like PEG-6000 in place of a hydrophilic carrier like PEG-6000, as mannitol is already part of a fixed-dose combination with celecoxib, thus obviating the need for an additional excipient.

Further in-vitro drug release studies were conducted for PEG-6000; however, there was no significant difference in the t90% between pure drug, physical mixture, or solid dispersion forms of mannitol. Based on these findings, the formulations PMPG2 and PMPG3 were selected for further investigation.

Differential Scanning Calorimetry Study of Celecoxib & Mannitol, PMPG2 and PMPG3

The selected batches, PMPG2 and PMPG3, were subjected to physical characterization through Differential Scanning Calorimetry (DSC) to confirm the amorphization of crystalline Celecoxib. The pure Celecoxib drug and PEG-6000 were also tested as controls. The peaks observed in the DSC thermograms for each formulation are summarized in Table 6.

The DSC thermogram of Celecoxib pure drug", PEG-6000, and SDPMPG2 reveals distinct endothermic peaks at 266°C, 168°C, and 120°C, respectively. The endothermic peak corresponding to the melting of Celecoxib at 266°C in the DSC thermogram of pure Celecoxib was notably absent in the DSC thermogram of solid dispersion SDPMPG3. Similarly, for SDPMPG3, the DSC thermogram showed endothermic peaks at 266°C for Celecoxib and 160°C for PEG-6000. Again, the melting peak of Celecoxib observed at 266°C in the pure drug was absent in the DSC thermogram of the solid dispersion SDPMPG3.

The absence of the endothermic peak associated with the melting of Celecoxib in both SDPMPG2 and SDPMPG3 likely indicates that Celecoxib has been converted into its amorphous form within the solid dispersion. This could also be due to the dissolution of crystalline Celecoxib in the molten carrier, resulting in the absence of the characteristic melting point, a common indicator of amorphization or solubilization in the formulation process. This amorphization of Celecoxib is expected to contribute significantly to the improvement in solubility and dissolution rate, as the amorphous form typically dissolves more readily than the crystalline form.

X-Ray Diffraction Study of Celecoxib Pure Drug, SDPMPG2, and SDPMPG3

Celecoxib pure drug, SDPMPG2, and SDPMPG3 were analyzed using X-Ray diffraction (XRD) to validate the results obtained from the DSC study. The X-Ray diffractograms, and the characteristic peaks are listed in Tables 7–8.

In the XRD pattern of Celecoxib pure drug, distinct sharp peaks were seen at diffraction angles (2θ) of 10.749°, 16.714°, 18.279°, 16.61°, 20.61°, 20.97°, and 23.03°, indicating its crystalline nature. In contrast, the XRD of SDPMPG3 showed peaks at diffraction angles (2θ) of 10.749°, 12.01°, 14.42°, and 19.8°, while the diffractogram of PMPG3 revealed peaks at 12.4°, 20.61°, and 27.72°, corresponding to PEG-6000, along with other peaks of lower intensity. These observations suggest that only a few of the crystalline peaks of Celecoxib were still present in the solid dispersions.

The peak intensities in the solid dispersion were significantly lower compared to the pure Celecoxib drug. Furthermore, the total number of crystalline peaks observed in the XRD of Celecoxib pure drug was 32, while only 18 peaks were seen in PMPG3, and 15 peaks in SDPMPG3. The percentage crystallinity was found to be 42.86% for SDPMPG2 and 50.82% for SDPMPG3, as shown in Table 7. The reduced peak count, decreased peak intensity, and lower percentage of crystallinity all point to the amorphization of a significant portion of Celecoxib in the solid dispersions.

However, a small fraction of Celecoxib remained in its crystalline form. The observed enhancement in the dissolution rate of Celecoxib from the solid dispersions is likely due to the amorphization of the crystalline drug in PEG-6000. This could also be attributed to improved wettability, dispersibility, particle size reduction, and an increased surface area of the drug.

FT-IR STUDIES

To further investigate potential interactions between the drug and the polymeric carrier, infrared spectra were recorded. Four distinct spectra were obtained for each of the drugs analyzed, which included: the drug alone, the polymer alone, the physical mixture of the drug with the polymer, and the solid dispersion of the drug with the polymer.

FTIR spectra of polymer alone, celecoxib alone, solid dispersion, and physical mixture of celecoxib and PEG-6000:

The infrared spectra of the polymer exhibited sharp peaks at 3400 cm-1, 1750 cm-1, and 1400-1350 cm-1, which correspond to the stretching vibrations of O-H, C=O, and C-O-C groups, respectively. The FTIR spectra of celecoxib showed sharp transitions at 3314.55 cm-1, 2914.06 cm-1, 1768.45 cm-1, 1688.10 cm-1, 1255.73 cm-1, 962.26 cm-1, and 749.31 cm-1, which correspond to bond stretches related to N-H, O-H, C=O (carboxylic group), C=O (ketonic group), C-C ring deformation, and C-H bonds, respectively.

Analysis of the spectra for both the solid dispersion (Figure 4) and the physical mixture of celecoxib loaded with PEG-6000 (Figure 5) revealed a sharp peak at 1760 cm-1, corresponding to the C=O stretching for celecoxib at 1700 cm-1 and the carboxylic group at 1650 cm-1, as discussed in the literature. These observations indicate that no significant changes were observed in the specific absorption bands of both the polymer and the drug, suggesting that there is no interaction between the two components.

Scanning electron microscopy (SEM) Studies

SEM images at various magnifications were employed to explore the morphological differences of the samples, including the drug, PEG-6000, physical mixtures, and solid dispersions. Figure 6 presents the SEM images of PEG-6000 and Celecoxib, which display irregularly shaped structures.

6.2.1 SEM of Celecoxib, solid dispersion and physical mixture of Celecoxib- PEG-6000

The figure demonstrates that Celecoxib, as seen in SEM image Figure 7 (A), consists of irregularly shaped particles. In the physical mixture of Celecoxib with PEG-

6000, shown in Figure 7 (B), the drug appears to be attached to the surface of the carrier. The SEM of the solid dispersion in Figure 7 (C) suggests that the drug is likely dispersed within the carrier matrix, further supporting the findings from the DSC analysis.

Evaluation of Flow Properties of Solid Dispersions of Celecoxib

Following the evaluation of the solid dispersions for their in-vitro dissolution and solid-state characterization, the same solid dispersions were assessed for their flow properties. The results of the blend characteristics are summarized in Table 10 below:

6.2.2 Evaluation of flow properties of prepared granules of solid dispersions of Celecoxib:

Due to the poor flow properties observed in the selected batches of solid dispersions SDPMPG2 and SDPMPG3, as shown in Table 11, these batches were then subjected to tablet formulation. The prepared granules were subsequently evaluated for their flow properties. Parameters such as Angle of Repose, Compressibility Index, and Hausner's Ratio were determined.

Evaluation of Physical Parameters of Prepared Tablets of Solid Dispersions of Celecoxib

The prepared tablets, TSDPMPG2 and TSDPMPG3, were evaluated for various physical parameters such as hardness, weight variation, friability, disintegration time, and drug content, and were found to be satisfactory. The hardness of the tablets ranged from 4.89 ± 0.26 kg/cm² in TSDPMPG2 to 4.56 ± 0.12 kg/cm² in TSDPMPG3. The friability values ranged from 0.89% in TSDPMPG2 to 0.66% in TSDPMPG3. Disintegration times varied between 5.15 minutes in TSDPMPG2 and 4.58 minutes in TSDPMPG3. The average tablet weights ranged from 77.12 ± 5.54 mg in TSDPMPG2 to 131.47 ± 3.38 mg in TSDPMPG3. All 20 tablets weighed were within the specified limits of ± 7.5%, meeting the weight variation test as per I.P. The average drug content was found to be 25.13 ± 0.79% in TSDPMPG2 and 25.49 ± 0.95% in TSDPMPG3, with all 10 tablets analyzed containing drug content within 85 to 115% of the average. Therefore, both batches passed the uniformity of drug content test. All parameters were within the specified limits, as summarized in Table 12.

***In-Vitro* Dissolution Study of Tablets of Solid Dispersion of Celecoxib**

The tablets were subsequently subjected to in-vitro drug dissolution studies as described earlier. The dissolution profiles of the tablets were found to be comparable to the solid dispersions. The t90% values for TSDPMPG2 and TSDPMPG3 were 42.48 minutes and 51.75 minutes, respectively. In comparison, the t90% for the marketed formulation was 96.46 minutes. The results demonstrated a significant ($p < 0.001$) enhancement in the dissolution rate of Celecoxib from the prepared tablets of solid dispersions, compared to the marketed tablet. The in-vitro drug dissolution data is presented, and the comparative in-vitro drug release profiles are shown in Figure 8.

Stability Study of Optimized Formulation

The tablet TSDPMPG2 was chosen for stability studies due to its lower weight and reduced polymer content. The results indicated that TSDPMPG2 remained stable based on its physical characteristics (color) and the percentage of drug release over 180 days under accelerated storage conditions. This suggests that TSDPMPG2 is the most promising formulation in the current study.

The developed formulations remained stable for 6 months at 40±2ºC/75±5% RH. No alterations in the physical appearance of the formulation were noted during the stability studies. Additionally, there were no significant changes in the Z-average size, PDI, or zeta potential, as analyzed using Student's t-test. Therefore, it can be concluded that the efavirenz SLN formulations were stable under both long-term and accelerated stability conditions (40 ± 2ºC/75 ± 5% RH) for 6 months.

Conclusions

For drugs with lower water solubility, the dispersion of solids in hydrophilic carriers can be regarded as a highly significant factor in improving the rate of dissolution. The solid dispersion method improves the drug's solubility in both the organic and aqueous phases. The crystalline drug particles are transformed into an amorphous form during the solid dispersion formulation process, which results in a reduction in particle size and an increase in particle surface area.

Infrared spectra of celecoxib showed sharp characteristic peaks 1714.71cm-1 and 3315.53 cm-1 assigned to $C_{10}O_{11}$ and O-H stretching vibrations respectively, display a downward due to intermolecular hydrogen bond type interactions. The DSC thermogram of Celecoxib exhibited a sharp endothermic peak at 136°C, while PVP K-30, Mannitol, and PEG-6000 displayed broad endothermic peaks, indicating their amorphous nature. The DSC thermogram of PEG-6000 showed a sharp endothermic peak at 62.73°C.

The SEM of PEG-6000 and Celecoxib showed irregularly shaped particles. Solid dispersions prepared using the microwave method with PEG-6000, Polyvinylpyrrolidone K-30, and Mannitol exhibited no detectable Celecoxib peak. This absence of the Celecoxib peak in the solid dispersions could be attributed to the molecular dispersion of the drug within the polymer, leading to the conversion of Celecoxib from its crystalline form to an amorphous form, which was confirmed by XRD and SEM studies.

The X-ray diffractogram of Celecoxib displayed sharp peaks at diffraction angles (2θ) of 7.6°, 10°, 13°, 15°, 16.5°, 20.1°, 22.6°, 25.25°, and 30.5°, indicating its crystalline nature.

The prepared solid dispersions were further evaluated for drug content, production yield, solubility, and dissolution studies. Drug content analysis showed that 85–115% of the drug was uniformly incorporated into the solid dispersions, indicating uniform drug distribution. The production yield was above 95% for all solid dispersion batches, except for those prepared via solvent evaporation and spray drying methods. Solubility studies indicated that

the solid dispersions prepared with PEG-6000 significantly enhanced the solubility of Celecoxib compared to the pure drug. The solubility enhancement is likely due to the reduction in polymer viscosity, decreased crystallinity of the drug, and the wetting, solubilizing, and surface-active properties of the polymers.

All prepared batches passed the weight variation test (within 90-110%) and showed friability of less than 1%. Tablets from batches TSDPMPG2 and TSDPMPG3 disintegrated faster than the other batches. Drug content was within the specified range (95–105%) for all batches. The dissolution profile of plain Celecoxib immediate-release tablets was compared with TSDPMPG2 and TSDPMPG3 tablets. The results showed significant enhancement in the dissolution rate with the solid dispersion tablets. The highest drug release was observed with TSDPMPG2 and TSDPMPG3 tablets. Therefore, batch TSDPMPG2 was selected for stability testing. The stability study of batch TSDPMPG2 revealed that the optimized immediate-release tablet remained stable over a period of six months.

References

1. Tiwary AK. Modification of crystal habit and its role in dosage form performance. Drug development and industrial pharmacy. 2001 Jan 1;27(7):699-709.
2. Uekama K. Design and evaluation of cyclodextrin-based drug formulation. Chemical and pharmaceutical bulletin. 2004;52(8):900-15.
3. Uekama K, Hirayama F, Arima H. Recent aspect of cyclodextrin-based drug delivery system. Journal of inclusion phenomena and macrocyclic chemistry. 2006 Oct;56:3-8.
4. Lawrence MJ, Rees GD. Microemulsion-based media as novel drug delivery systems. Advanced drug delivery reviews. 2000 Dec 6;45(1):89-121.
5. Sekiguchi K, Obi N. Studies on Absorption of Eutectic Mixture. I. A Comparison of the Behavior of Eutectic Mixture of Sulfathiazole and that of Ordinary Sulfathiazole in Man. Chemical and Pharmaceutical Bulletin. 1961 Nov 25;9(11):866-72.
6. Sekiguchi K, Obi N, Ueda Y. Studies on Absorption of Eutectic Mixture. II. Absorption of fused Conglomerates of Chloramphenicol and Urea in Rabbits. Chemical and Pharmaceutical Bulletin. 1964 Feb 25;12(2):134-44.
7. Nogami H, Nagai T, Suzuki A. Studies on powdered preparations. XVII. Dissolution rate of sulfonamides by rotating disk method. Chemical and Pharmaceutical Bulletin. 1966 Apr 25;14(4):329-38.
8. Saffoon N, Uddin R, Huda NH, Sutradhar KB. Enhancement of oral bioavailability and solid dispersion: a review. Journal of Applied Pharmaceutical Science. 2011 Sep 30(Issue):13-20.
9. Owusu-Ababio G, Habib MJ. Polymers applied in solid dispersion technology. Clinical research and regulatory affairs. 1998 Jan 1;15(1):25-45.
10. Torrado S, Torrado S, Torrado JJ, Cadórniga R. Preparation, dissolution and characterization of albendazole solid dispersions. International journal of pharmaceutics. 1996 Aug 30;140(2):247-50.
11. Almarsson Ö, Zaworotko MJ. Crystal engineering of the composition of pharmaceutical phases. Do pharmaceutical co-crystals represent a new path to improved medicines?. Chemical communications. 2004(17):1889-96.
12. Trask AV, Motherwell WS, Jones W. Solvent-drop grinding: green polymorph control of cocrystallisation. Chemical Communications. 2004(7):890-1.
13. Ruscic B, Pinzon RE, Morton ML, von Laszevski G, Bittner SJ, Nijsure SG, Amin KA, Minkoff M, Wagner AF. Introduction to active thermochemical tables: Several “key” enthalpies of formation revisited. The Journal of Physical Chemistry A. 2004 Nov 11;108(45):9979-97.
14. Valvanix SC, Yalkowsky SH, Roseman TJ. Solubility and partitioning IV: Aqueous solubility and octanol-water partition coefficients of liquid nonelectrolytes. Journal of pharmaceutical sciences. 1981 May 1;70(5):502-7.
15. Jain P, Yalkowsky SH. Solubilization of poorly soluble compounds using 2-pyrrolidone. International journal of pharmaceutics. 2007 Sep 5;342(1-2):1-5.
16. Valizadeh H, Nokhodchi A, Qarakhani N, Zakeri-Milani P, Azarmi S, Hassanzadeh D, Löbenberg R. Physicochemical characterization of solid dispersions of indomethacin with PEG 6000, Myrj 52, lactose, sorbitol, dextrin, and Eudragit® E100. Drug development and industrial pharmacy. 2004 Jan 1;30(3):303-17.
17. Barzegar-Jalali M, Maleki N, Garjani A, Khandar AA, Haji-Hosseinloo M, Jabbari R, Dastmalchi S. Enhancement of dissolution rate and anti-inflammatory effects of piroxicam using solvent deposition technique. Drug development and industrial pharmacy. 2002 Jan 1;28(6):681-6.
18. Jerome MP, Alahmad FA, Salem MT, Tahir M. Layered double hydroxide (LDH) nanomaterials with engineering aspects for photocatalytic CO2 conversion to energy efficient fuels: Fundamentals, recent advances, and challenges. Journal of Environmental Chemical Engineering. 2022 Oct 1;10(5):108151.
19. Wang Y, Zhang D, Du G, Du R, Zhao J, Jin Y, Fu S, Gao L, Cheng Z, Lu Q, Hu Y. Remdesivir in adults with severe COVID-19: a randomised, double-blind, placebo-controlled, multicentre trial. The lancet. 2020 May 16;395(10236):1569-78.
20. Mazzola L, Faillenot I, Barral FG, Mauguière F, Peyron R. Spatial segregation of somato-sensory and pain activations in the human operculo-insular cortex. Neuroimage. 2012 Mar 1;60(1):409-18.
21. Wang H, Li Q, Reyes S, Zhang J, Xie L, Melendez V, Hickman M, Kozar MP. Formulation and Particle Size Reduction Improve Bioavailability of Poorly Water-Soluble Compounds with Antimalarial Activity. Malaria Research and Treatment. 2013;2013(1):769234.
22. Wang J. Effects of particle size and morphology on filtration of airborne nanoparticles. KONA Powder and Particle Journal. 2013;30:256-66.

23. Pouton CW. Formulation of poorly water-soluble drugs for oral administration: physicochemical and physiological issues and the lipid formulation classification system. European journal of pharmaceutical sciences. 2006 Nov 1;29(3-4):278-87.
24. Vasconcelos T, Sarmento B, Costa P. Solid dispersions as strategy to improve oral bioavailability of poor water soluble drugs. Drug discovery today. 2007 Dec 1;12(23-24):1068-75.
25. Wei M, Xiong Y, Zhang L, Li J, Peng PA. The effect of sample particle size on the determination of pore structure parameters in shales. International Journal of Coal Geology. 2016 Jun 1;163:177-85.
26. Zhang S. Impacts of polymorphism and selected polymers on the recrystallization of amorphous itraconazole. The Chinese University of Hong Kong (Hong Kong); 2017.
27. Mistry P, Amponsah-Efah KK, Suryanarayanan R. Rapid assessment of the physical stability of amorphous solid dispersions. Crystal Growth & Design. 2017 May 3;17(5):2478-85.
28. Frank DS, Matzger AJ. Effect of polymer hydrophobicity on the stability of amorphous solid dispersions and supersaturated solutions of a hydrophobic pharmaceutical. Molecular pharmaceutics. 2019 Jan 15;16(2):682-8.